Scientia Iranica (2024) 31(21), 2056–2070

Sharif University of Technology
Scientia Iranica
Transactions D: Computer Science & Engineering and Electrical Engineering
https://scientiairanica.sharif.edu

Research Note

A novel robust model reference adaptive MPPT controller for Photovoltaic systems

Saibal Manna[a,*], Deepak Kumar Singh[a], Ashok Kumar Akella[a], Almoataz Y. Abdelaziz[b], and Miska Prasad[c]

a. *Department of Electrical Engineering, NIT Jamshedpur, Jharkhand-831014, India.*
b. *Faculty of Engineering and Technology, Ain Shams University, Cairo-11517, Egypt.*
c. *Department of Electrical & Electronics Engineering, ACE Engineering College, Telangana-501301, India.*

Received 15 December 2021; received in revised form 28 February 2022; accepted 15 August 2022

KEYWORDS
Photovoltaic;
MPPT;
DC-DC converter;
Robust model reference adaptive MPPT controller;
MIT rule;
OPAL-RT.

Abstract. Solar photovoltaic (SPV) power generation has been more popular throughout the world in recent years due to its recyclable and eco-friendly nature. As a result, extracting the maximum power from SPV systems is important. Our contribution to this problem is to harvest maximum power under changes in ambient conditions and parametric variations. This paper presents a novel robust model reference adaptive maximum power point tracking controller (RMRAC-MPPT) for PV systems under five different cases including temperature, load, irradiance, boost converter capacitance, and inductance variations. To assess the robustness of the proposed method, MATLAB/Simulink software is used to compare it to the state-of-the-art techniques such as INC, P&O, FLC, AFLC, SMC, back stepping-SMC, PI, iRCS-MPC, P&O-MPC, ANFIS, BAT-FLC, and IPID. The verification of the proposed method is also tested in a laboratory-based OPAL-RT real-time simulator. It is evident that the proposed MPPT technique improves Maximum Power Point Tracking (MPPT) capabilities while reducing steady-state oscillations. Furthermore, with five different parameter variations, the time duration to capture Maximum Power Point (MPP) is 1.5 ms, which is significantly faster than other state-of-the-art techniques. In addition, the proposed technique has a tracking efficiency of 99.75% and an overall system efficiency of 96%.

1. Introduction

The world's energy demands are rapidly growing. This has resulted in excessive fossil fuels usages, which has had significant environmental implications such as ozone layer depletion, global warming, and acid rain. Renewable energy would be a possible solution to this crisis. Various renewable energy methods i.e., solar, wind, tidal, geothermal, etc. have been invented that are efficient and cost-effective as compared to traditional power generation. Solar energy is a significant

*. *Corresponding author.*
E-mail address: mannasaibal1994@gmail.com (S. Manna)

To cite this article:
S. Manna, D. Kumar Singh, A. Kumar Akella, A.Y. Abdelaziz, and M. Prasad "A novel robust model reference adaptive MPPT controller for Photovoltaic systems", *Scientia Iranica* (2024) **31**(21), pp. 2056-2070
https://doi.org/10.24200/sci.2022.59553.6312

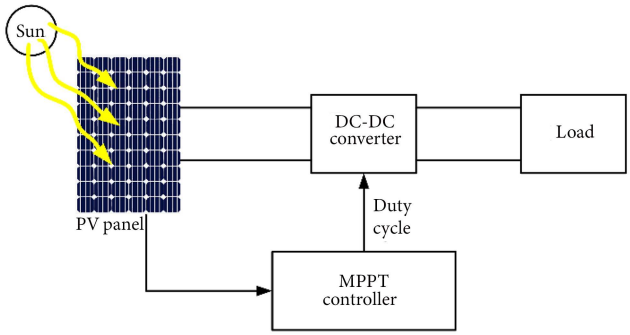

Figure 1. Typical block diagram of MPPT controller with PV system.

source of energy because of its worldwide accessibility, ease of installation, no noise, less maintenance and clean energy generation [1]. Solar photovoltaic (SPV) systems are used for a variety of purposes such as electric transportation, roadside lamps, remote power generation, commercial electricity generation, and solar-driven air conditioning system [2].

The key obstacles for solar power usage, which limit the amount of solar energy extracted, are atmosphere, temperature, dust, geographic areas, and cloud covering. On the other hand, rapid fluctuations in solar temperature and radiation have a negative impact on the PV system's performance. Due to these changes, PV systems cannot offer maximum power to the load indefinitely. As a result, algorithm like Maximum Power Point Tracking (MPPT) is required to quickly adjust the PV system for changing climate conditions and supply optimal power to the load [3]. The main goals of MPPT are to ensure fast, precise maximum power tracking and reduce oscillations. Boost converter is best suited to PV applications, as it allows low inductivity to eliminate current ripples and has lower switching losses. Under changeable weather circumstances, MPPT techniques modify the dc-dc converter duty cycle to transmit maximum power generated from the PV source to the grid or load. The basic block diagram of a typical MPPT controller used in a PV system is illustrated in Figure 1.

1.1. Literature review

Many MPPT approaches have been introduced in the literature, each with a distinct level of complexity, tracking speed, cost-effectiveness, accuracy, and MPPT operating mechanism. Fundamental methodologies are devised using current, duty cycle, and voltage as well as PV cell mathematical model, and are used to estimate optimal operating points on the P-V curve. MPPT approaches may be divided into three types: Artificial Intelligence (AI), Indirect, and direct-based techniques [4].

Indirect MPPT approaches, such as Short Circuit Current (SCC) and Open-Circuit Voltage (OCV), rely on the performance characteristics of PV panels under a variety of environmental circumstances. The indirect techniques cannot provide exact tracking of Maximum Power Point (MPP) at any temperature and irradiance [5]. Further sophisticated MPPT algorithms are called direct techniques. The most often utilized direct approaches are Perturb and Observe (P&O) and incremental conductance (INC). The P&O algorithm is well-known for its simplicity, low operational costs, and easy to implement. However, its shortcomings, such as incorrect tracking direction with a sudden increase in irradiance and seems significant fluctuations near MPP, become significant obstacles [6]. Another direct MPPT method is INC, which delivers better outcomes in terms of efficiency, speed, and accuracy as compared to P&O. Furthermore, during a considerable variation in solar irradiation, the P&O and INC may not offer the speed and accuracy necessary to attain the MPP [7].

AI-based MPPT techniques, including Particle Swarm Optimization (PSO) [8], Fuzzy Logic Control (FLC) [9], Artificial Neural Networks (ANN) [10], and Genetic Algorithm (GA) [11], give better tracking performance and efficiency under rapidly fluctuating climate conditions. However, compared to traditional techniques, these MPPT algorithms are more difficult and expensive to apply. A variety of hybrid MPPT approaches such as INC-based FLC [12], BAT-FLC [13], etc. have been proposed to combine the advantages of two different MPPT techniques and solve the problem to maintain MPP.

Extensive research has been done in the literature to alleviate the disadvantages of existing techniques. A SOFT (steady output & fast tracking)-MPPT algorithm is developed, which attempts to improve the tracking and steady-state performance of both INC and P&O algorithms. To follow the MPP, an adaptive step size is employed, which gives a faster tracking response. The experimental and simulation outcome have validated the algorithm performance under uniform climate situations [14]. To overcome the shortcoming of the standard P&O method, a coarse and fine control approach is introduced. This concept offers three control states, each with its own specific features. States 1 and 2 improve tracking speed whereas state 3 regulates steady-state oscillations. The simulated comparison study shows that the new approach has lower oscillations, greater tracking efficiency, faster-tracking speed, lower power loss compared to other strategies [15]. To enhance the PV system's performance, an adjustable variable step backstepping (VS-BS) MPPT approach is presented. The approach is a two-level hybrid MPPT technique that combines VS-P&O and BS controller. The goal of merging two independent MPPT approaches is to improve tracking accuracy and speed while maintaining a simple scheme [16]. A robust Sliding Mode Controller (SMC) is introduced to track the MPP under solar radiation and temperature

Table 1. Comparison of the various MPPT techniques.

MPPT method	Complexity	Steady-state oscillation	Efficiency	Convergence speed	Climate change and parameter variations
Modified FLC [4]	Medium	No	High	Fast	I & T
SOFT-MPPT [14]	Low	No	Very high	Fast	Only I
Coarse and fine MPPT [15]	Low	No	High	Fast	I, T & R individually
VS-BS [16]	Medium	No	Very high	Fast	I & T
FPIDN MPPT [19]	High	No	Very high	Fast	I & T
BS-SMC [22]	High	No	Very high	Fast	I & T
Improved restricted control set model (iRCS)-MPC [23]	High	No	High	Very fast	Only I
BAT-FLC [24]	High	No	Very high	Fast	I & T
IPID-MPPT [25]	High	No	Very high	Fast	Only I
Proposed MPPT	**Medium**	**No**	**Very high**	**Very fast**	**I, T, L, BI, and BC**

I: Irradiation, T: Temperature, R: Load, BI: Boost converter Inductance, BC: Boost converter Capacitance

variations. In addition, the hysteresis quantized input is considered to overcome the chattering problem in traditional SMC [17]. A new MPPT approach based on Adaptive FLC (AFLC) is described. The Grey Wolf Optimization (GWO) approach is used to optimize the AFLC membership function. The suggested method follows global MPP under all shading situations and improves efficiency, tracking time, and, oscillations [18]. A filter-based adaptive Fuzzy Proportional Integral Derivative (FPIDN) controller for MPPT is implemented. The suggested MPPT's efficacy has been compared to other MPPT approaches like AFLC, FLC, INC, and P&O. The new controller efficiency is between 99.45%–99.72% with MPP capture time at 0.048 s under changing temperature and radiation conditions [19]. An asymmetrical FLC are proposed to track the global MPP under changing radiation and temperature conditions [20]. Under varying climate conditions like temperature and radiation, an Adaptive Neuro-Fuzzy Inference System (ANFIS)-based MPPT controller for a standalone PV system is presented. The suggested controller can follow the MPP quicker than FLC and P&O under changing weather conditions [21]. Using FLC, an updated MPPT technique has been devised. Under varying temperature and radiation circumstances, the suggested method's accuracy ranges between 99.5% to 99.9%. Furthermore, the duration to capture MPP is 21 ms. It is approximately five times and four times faster than INC and P&O respectively [4].

As per the literature survey, most of the proposed MPPT controllers are working under both temperature and radiation conditions only. These MPPT algorithms, on the other hand, are not discussed other parameter variations like load, boost converter inductance, and capacitance. Moreover, the time to follow the MPP is not so much impressive. In this paper, a novel robust model reference adaptive MPPT controller (RMRAC) is proposed for PV systems under five different cases including temperature, radiation, load, boost converter capacitance as well as inductance. Furthermore, MATLAB simulation results, as well as laboratory-based OPAL-RT real-time simulator validation, were performed to confirm the effectiveness of the proposed control scheme. Additionally, the time duration to capture MPP is 1.5 ms under five different parameter variations which is much lower than other well-known techniques. The proposed method has 99.75% tracking and 96% overall system efficiency. Table 1 illustrates the comparison of various MPPT approaches.

The following are the primary contributions of the proposed research:

- To design and implementation of a novel robust model reference adaptive controller for MPPT application focused on boost converter;
- To evaluate the robustness of the proposed controller, five different cases are considered: temperature, load, solar irradiation, boost converter capacitance as well as inductance variation;
- The proposed controller results are compared with the state-of-the-art technique such as INC, P&O, FLC, Adaptive FLC, SMC, back stepping-SMC, PI, iRCS-MPC, P&O-MPC, ANFIS, BAT-FLC, and IPID in terms of tracking speed and efficiency;

- MATLAB/Simulink software is used to compare various state-of-the-art MPPT approaches for assessing its resilience;
- Real-time validation using the OPAL-RT simulator (OP-4510) further proves the applicability of the suggested method in the real world.

Four key sections are included in this paper: Section 2 addresses the PV system mathematical model. Boost converter dynamics and integration with PV systems are addressed in Section 3. The MRAC design procedure is explained in Section 4. Section 5 provides the simulation result of the research. Section 6 gives the concluding remark of the paper.

2. PV mathematical model

The PV cell's most common model is made up of parallel and series resistors attached to a current source and a diode displayed in Figure 2. R_{pe} and R_{se} denote parallel and series resistance [4].

The equation for the solar cell's output current is:

$$I = I_R - I_{d1} - I_{pe}, \tag{1}$$

where I_R displays photo current without loss and depends on solar temperature and irradiance. I_{d1}, I, and I_{pe} represent diode, output, and parallel resistance leakage current respectively.

$$I_{d1} = I_{01}(e^{q.\frac{(V+I\,R_{se})}{nKT}} - 1). \tag{2}$$

where I_{01}, n, q, T, and K reflect reverse saturation current, diode factor, electron charge, p-n junction temperature, and Boltzmann constant respectively. The basic equation for current produced in PV cell is presented in Eq. (3):

$$I_R = \frac{W}{W_0}\left(I_c + \lambda(t - t_0)\right), \tag{3}$$

where I_c represents SCC. W and W_0 are irradiances and reference irradiance during the day while t and t_0 are temperature and reference temperature during the day. λ is the temperature coefficient:

$$I = I_R - I_{01}\left[e^{q.\frac{(V+I\,R_{se})}{nKT}} - 1\right] - \frac{V + R_{se}I}{R_{pe}}. \tag{4}$$

The I_{01} is defined by:

$$I_{01} = I_{01ref}\left(\frac{t}{t_0}\right)^3 e^{\left[(\frac{qE_G}{nK})(\frac{1}{t}-\frac{1}{t_0})\right]}, \tag{5}$$

where E_G is the energy bandgap. Table 2 displays the specification of the PV panel adopted in this research.

More specifically, as displayed in Figure 3, the MPP changes with ambient conditions, and a controller is required to set the PV power close to the MPP. The method of the controller design relies essentially on the modeling of PV cells for the interface with environmental conditions.

The MPP exists when the rate of change of power with respect to voltage is zero, as illustrated in Figure 3(b). and it is expressed as in Eq. (6):

$$\frac{dP}{dV_{PV}} = \begin{cases} = 0, & \text{at } MPP \\ > 0, & \text{at left side of } MPP \\ < 0, & \text{at right side of } MPP \end{cases} \tag{6}$$

Table 2. Solar module 1Soltech 1STH-215-P specification.

Parameter	Value
Maximum power	213.15 W
Maximum voltage	29 V
Maximum current	7.35 A
Open circuit voltage	36.3 V
Short circuit current	7.84 A

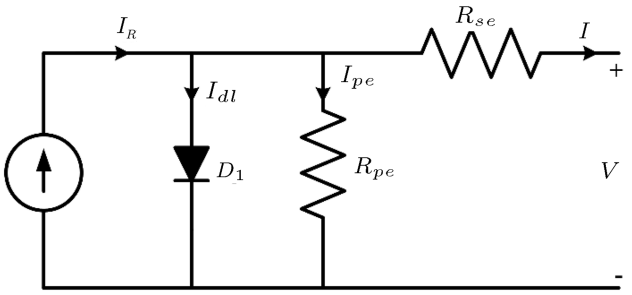

Figure 2. Equivalent circuit of a solar cell.

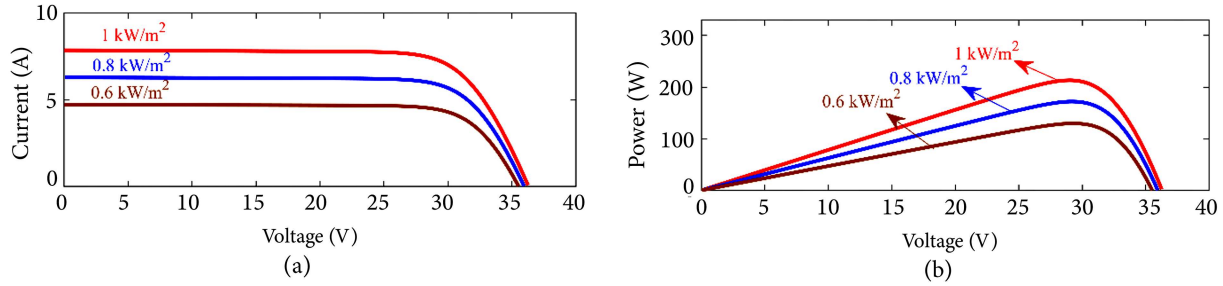

Figure 3. The impact of the environmental conditions on current and power values. (a) I–V and (b) P–V curves for various radiation values at 25°C.

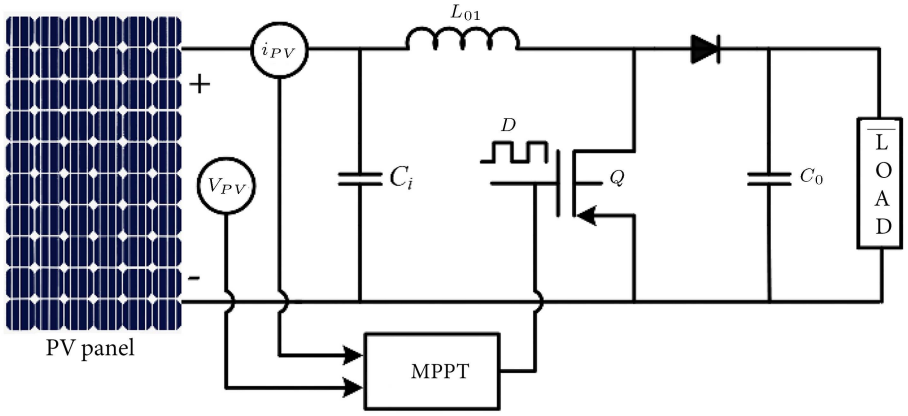

Figure 4. PV system with boost converter and MPPT controller.

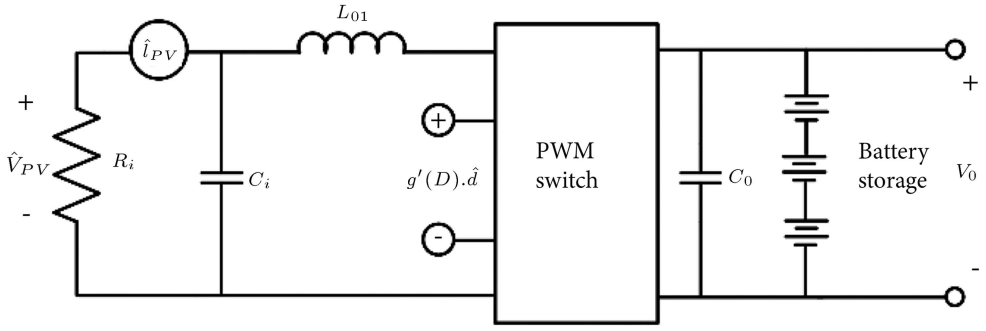

Figure 5. Small signal equivalent circuit of PV power conversion system.

For the MPPT adaptive controller, this Eq. (6) will be used as the control rule.

3. Boost converter dynamics

Figure 4 illustrates the incorporation of a device where a boost converter is used to supply maximum power to load. The boost converter model in Figure 5 shows the MPPT controller senses solar current and voltage and provides the duty cycle (D) to the switch Q. The D is connected to the array voltage through Eq. (7):

$$v_{PV} = i_{PV} R_0 (1 - D)^2, \tag{7}$$

where i_{PV} and v_{PV} are array current and voltage respectively. R_0 is the load resistance. Both array current and voltage contain dc (I_{PV} and V_{PV}) and ripple ($\hat{\imath}_{PV}$ and $\hat{v}_{PV}$) terms. The purpose is then to create a controller, which measures the optimum value of the loop continuously, to ensure that I_{PV} tracks I_M (V_{PV} tracks V_M) to deliver the maximum power.

Eq. (7) gives the foundation for the traditional MPPT method to evaluate D in a steady state. The MPPT control must take into account dynamics between the array voltage and D to maximize transient reactions. As transient oscillations are undesirable and can contribute to device inefficiency, MPPT controls must reduce oscillations from the array voltage after adjusting D for changing atmospheric conditions. The boost converter detailed dynamic model is discussed in Ref. [26]. A small-signal equivalent circuit is assumed to simplify the study of transient response as indicated in Ref. [27]. Figure 5 displays the small-signal equivalent circuit of PV. The solar array is modeled as resistor R_i, small-signal array current ($\hat{\imath}_{PV}$), and voltage ($\hat{v}_{PV}$) across its terminal.

Now Transfer Function (TF) of the control signal (D) to array voltage is derived around an operating point. This TF presents the system dynamics. The dynamic model in Figure 5 displays a battery load that is realistic for the PV system. Here, we neglect the battery dynamics in deriving the TF of array voltage to D in small-signal operations. We have the following relationship after analyzing Figure 5 [28]:

$$\frac{\hat{v}_{PV}(s)}{R_i} + s\hat{v}_{PV}(s)C_i = \frac{g'(D)\hat{d}(s) - \hat{v}_{PV}(s)}{sL_{01}}, \tag{8}$$

where $\hat{d}(s)$ reflects the small-signal variation around the D. $g(D)$ is the relation between D and V_{PV} while $g'(D)$ is the derivative of $g(D)$ with respect to D. From Eq. (8), we get:

$$\frac{\hat{v}_{PV}(s)}{\hat{d}(s)} = \frac{g'(D)}{L_{01}C_i s^2 + \frac{L_{01}}{R_i}s + 1}. \tag{9}$$

It is well known that:

$$g(D) = V_{PV} = (1 - D)V_0, \tag{10}$$

where V_0 is boost converter steady-state output. Eq. (10) assumes that V_0 and $g(D)$ are not influenced by transient switching behavior. From Eq. (10), $g'(D) = -V_0$ and now Eq. (9) will be:

$$\frac{\hat{v}_{PV}(s)}{\hat{d}(s)} = \frac{-\frac{V_0}{L_{01}C_i}}{s^2 + \frac{L_{01}}{R_iC_i}s + \frac{1}{L_{01}C_i}}. \tag{11}$$

The minus sign indicates that a reduction in the duty ratio raises the voltage of the panel. This study does not include the parasitic components of the power stage. The TF to above is calculated from a linearized version (as Figure 5) of a nonlinear system (as Figure 4), near a single operating point. The plant parameters C, L, and R are not constant and fluctuate within the lower and upper range of their nominal values (R^*, L^*, C^*) as:

$$R_{\min} \leq R^* \leq R_{\max}, \tag{12}$$

$$C_{\min} \leq C^* \leq C_{\max}, \tag{13}$$

$$L_{\min} \leq L^* \leq L_{\max}. \tag{14}$$

The goal is to ensure that the controller can handle a wide variety of load values (R) and also that the controller can work with varied boost converter sizes, which are represented by C and L. The ranges of values for each system parameter are displayed in Table 3.

To minimize current and voltage ripples, the boost converter inductance and capacitance values must be carefully chosen in the design. The capacitance is selected in such a way that the voltage ripples are minimized, as recommended in Ref. [26]:

$$C \geq \frac{1}{f\Delta V}D. \tag{15}$$

where ΔV and f are voltage ripple and switching frequency respectively. Estimating the voltage ripple factor as:

$$VRF = \frac{\Delta V}{V}. \tag{16}$$

The inductance is selected in such a way that the current ripples are minimized, as recommended in REf. [26]:

$$L \geq \frac{V}{f\Delta I}D(D-1), \tag{17}$$

where ΔI is the current ripple which is given as:

$$CRF = \frac{\Delta I}{I}, \tag{18}$$

where CRF is the current ripple factor.

Table 3. Ranges of values for the PV plant transfer function.

	R (Ω)	C (Farad)	L (Henry)
Nominal	20	2×10^{-4}	3×10^{-4}
Minimum	15	1×10^{-4}	2×10^{-4}
Maximum	35	3×10^{-4}	4×10^{-4}

4. Model reference adaptive control

The design of MRAC is presented to optimize the PV system output power. Figure 6 displays the overall schematic diagram of the proposed control scheme. A voltage-reference-based P&O algorithm is designed as the MPPT control scheme. Eq. (6) refers to the MPPT control law where maximum power exists and the reference voltage of the controller can vary as per the following equation, where V_{PV} is array voltage and ΔV is the small threshold voltage.

$$V_{ref} = \begin{cases} V_{PV}, \frac{dp}{dV_{pv}} = 0 \\ V_{PV} - \Delta V, \frac{dp}{dV_{PV}} < 0 \\ V_{PV} + \Delta V, \frac{dp}{dV_{PV}} > 0 \end{cases} \tag{19}$$

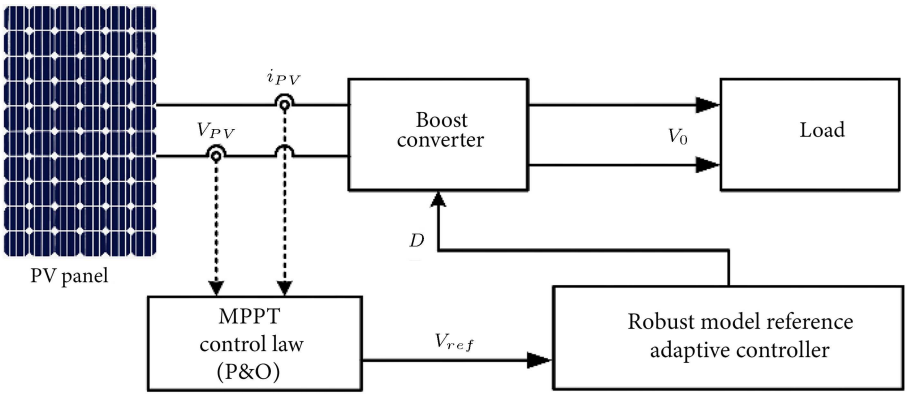

Figure 6. MPPT adaptive controller for PV system.

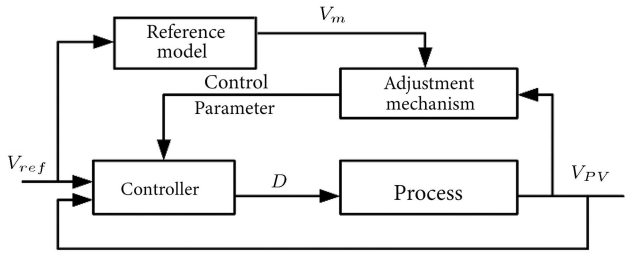

Figure 7. MRAC model.

The adaptive control technology can deal with uncertainties and disruptions in system structure, as well as changes in the operating conditions unless the feedback control. Due to its special characteristics and ease of execution, MRAC is designed for MPP applications. The MRAC required only reference and array voltage as input [29,30]. The MRAC primarily consists of a process, adaptation gain, and reference model as illustrated in Figure 7.

The key objective of MRAC is that the main process output should adopt the reference model output by use of adaptation gain. MRAC's design parameters are based on the choice of the reference model to indicate the optimal output response and a controller is designed to mitigate the error (e_z) between the model and plant output. To regulate the control law, adaptive control is used. The MIT law is one of the fundamental adaptive methods focused on a gradient strategy. This is the basic approach of the MRAC controller developed at MIT around 1960s for aerospace applications to minimize the e_z between the reference and system output by changing the adaptation laws to reduce cost function:

$$J(\phi) = \frac{{e_z}^2}{2}, \tag{20}$$

where e_z is the error between plant and reference model $e_z = V_{PV} - V_m$. The aim is to change the parameter to minimize $J(\varphi)$ in the direction of the negative gradient of J:

$$\frac{d\varphi}{dt} = -\eta \frac{\partial J}{\partial \varphi} = -\eta e_z \frac{\partial e_z}{\partial \varphi}, \tag{21}$$

where η is the adaptation gain, $\frac{\partial e_z}{\partial \phi}$ is system sensitivity and it is measured under the assumption that φ changes slowly. In the MRAC structure, the first-order model was chosen as follows:

$$\dot{x_m}(t) = A_m x_m(t) + B_m u_m(t). \tag{22}$$

The assumed model parameters are:

$$A_m = [4] \quad \text{and} \quad B_m = [4].$$

The control signal $D(t)$ is expressed as:

$$D(t) = \varphi_1 V_{ref}(t) - \varphi_2 V_{PV}(t), \tag{23}$$

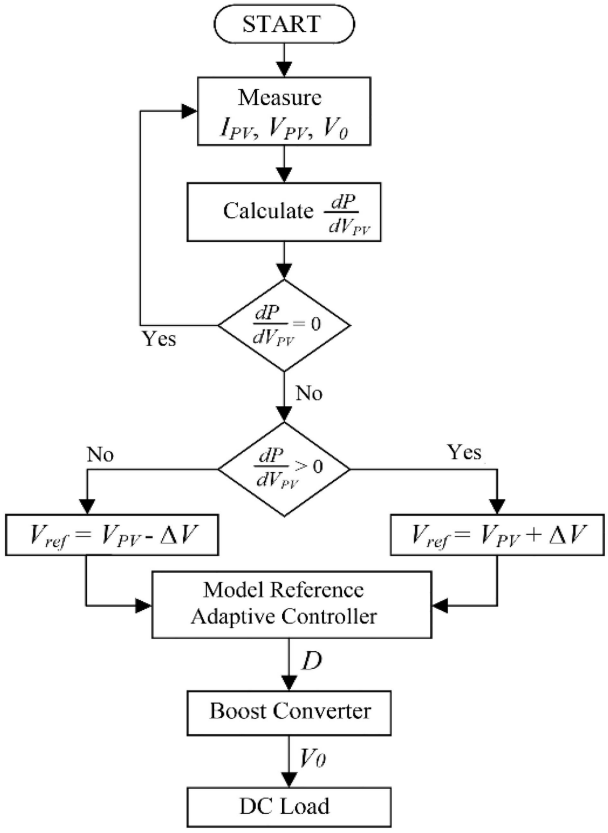

Figure 8. MRAC MPPT flowchart.

where the vector parameter $(\varphi) = [\ \varphi_1 \quad \varphi_2\ ]$. The adaptation law for MIT rule is:

$$\frac{d\varphi_1(t)}{dt} = -\eta \left(\frac{A_m}{p + A_m} V_{ref}(t) \right) e_z(t), \tag{24}$$

$$\frac{d\varphi_2(t)}{dt} = \eta \left(\frac{A_m}{p + a_m} V_{PV} \right) e_z(t), \tag{25}$$

where $p = \frac{d}{dt}$.

Now RMRAC controller design is completed, the next segment describes the results.

5. Result

The MPPT with RMRAC was simulated with the aid of the SIMULINK toolbox. The simulation comprises three major interconnected components: PV, Boost converter, and adaptive Controller model where the operating process is displayed in Figure 8. Considering the parameter value shown in Table 2. Here adaptation gain is considered as 0.08.

The PV cell maximum power (213.15 W) versus MPPT output power is shown in Figure 9 for 1000 W/m^2 radiation at 25°C. This finding illustrates that the reaction time of the MRAC adaptive controller is lower than 0.02 sec, which is quicker than any other controller as in [26,31]. Figure 10 shows the voltage

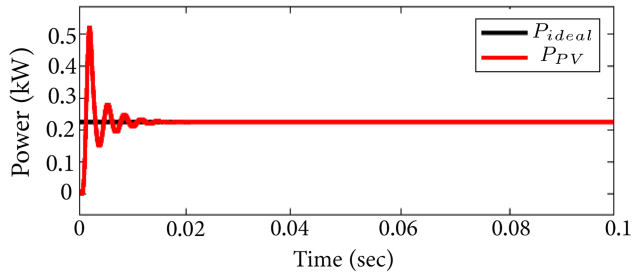

Figure 9. Ideal ($P_{\max}$) vs PV power (P_{pv}) for fixed 1000 W/m^2 at 25°C with $R_0 = 20\ \Omega$.

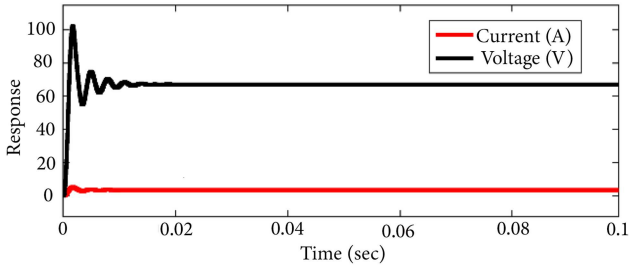

Figure 10. Current and voltage response for 1000 W/m^2 irradiance at 25°C with $R_0 = 20\ \Omega$.

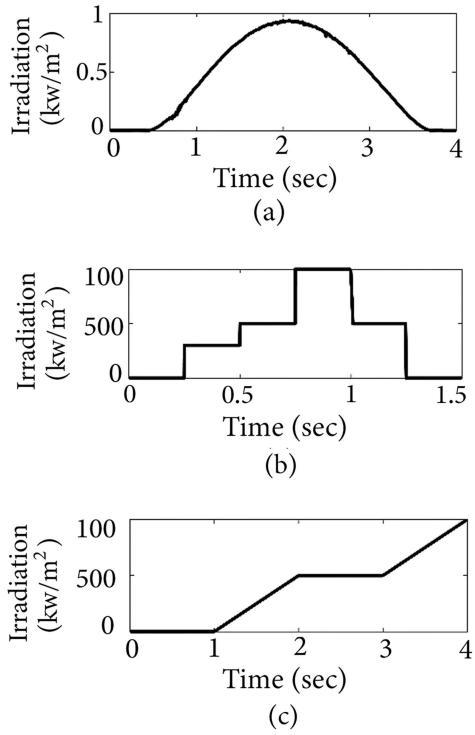

Figure 11. Different radiation curves under different weather conditions.

and current waveform. This adaptive controller will be able to track the MPP for any other solar radiation value easily.

In addition, the controller performance has been verified with various rapidly changing irradiation signals as shown in Figure 11. These variabilities can be described as distinct weather situations and are

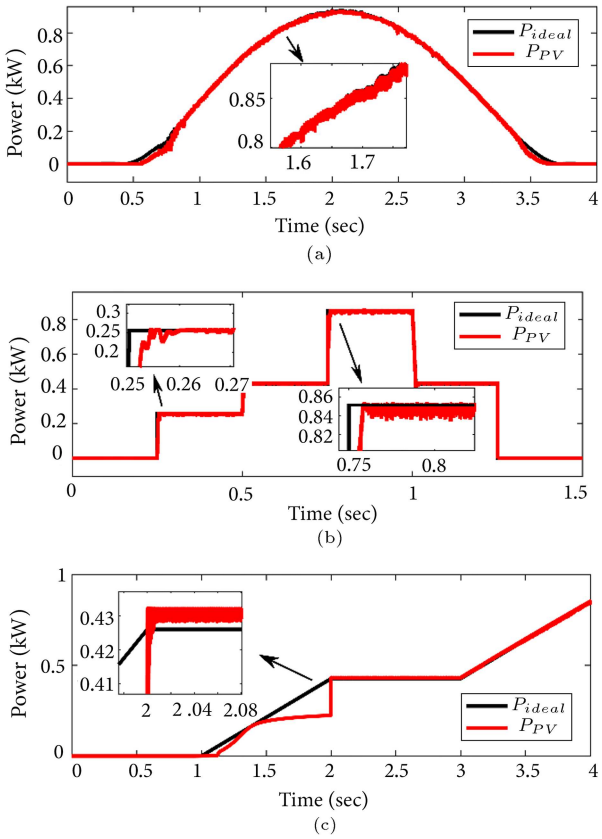

Figure 12. The ideal power and PV power under three different varying irradiation signals (in Figure 11, at 25 °C and $R_0 = 20\Omega$) using the P&O MPPT approach.

essential for validating the efficiency of the controller in cloudy or dusty weather.

The ideal power and PV power under three different varying irradiation signals (Figure 11) at constant temperature (25°C) with $R_0 = 20\ \Omega$ using normal P&O approach are shown in Figure 12. According to Figure 12 and its corresponding zoom view, it is clear that the P&O approach does not accurately track the ideal power under three different radiation signals.

The ideal power (P_{ideal}) and PV power (P_{PV}) under three different varying irradiation signals (Figure 11) at constant temperature (25°C) with $R_0 = 20\ \Omega$ using the proposed approach are shown in Figure 13. From Figure 13 and its zoom view, it is clear that the proposed approach accurately tracks the MPP compared to the traditional P&O approach with less oscillations. So, the proposed MPPT control is feasible under different rapidly changing radiation signals.

Now, the mentioned five different parameters are considered to check the robustness of the proposed approach. The irradiance, temperature, load, boost converter inductance, and capacitance signals are shown in Figure 14. The system operated in seven different states. State 1 is 1000 W/m^2, 25°C, 15 Ω, 0.4 mH, and 100 μF, State 2 is 1000 W/m^2, 30°C, 20 Ω, 0.4 mH, and 100 μF, State 3 is 800 W/m^2, 35°C, 20 Ω, 0.3 mH,

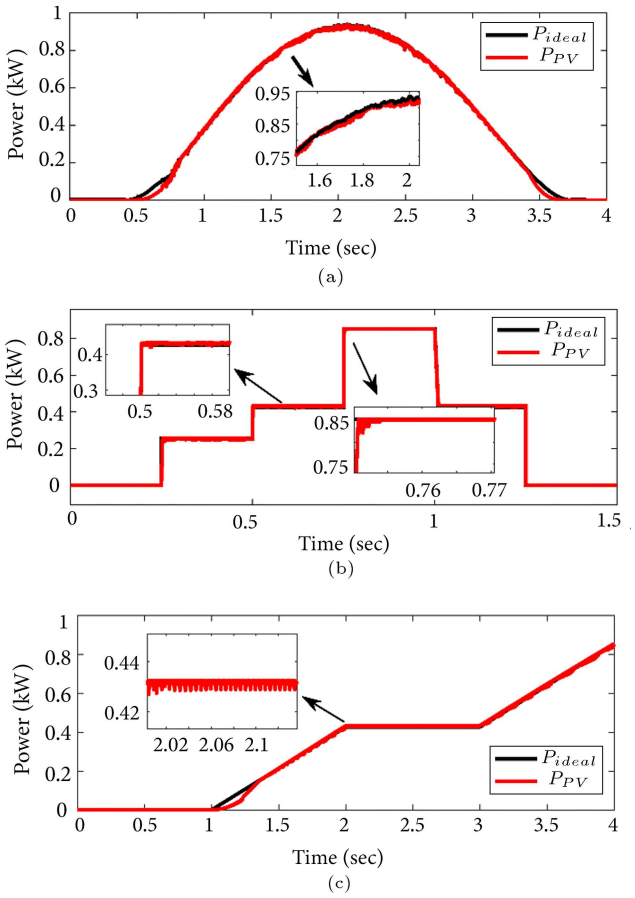

Figure 13. The ideal power and PV power under three different varying irradiation signals (in Figure 11, at 25°C and $R_0 = 20\ \Omega$) using proposed approach.

and 200 μF, State 4 is 800 W/m^2, 35°C to 20°C, 25 Ω, 0.3 mH, and 200–300 μF, State 5 is 600 W/m^2, 20°C to 35°C, 30 Ω to 35 Ω, 0.2 mH, and 300 μF to 100 μF, State 6 is 600 W/m^2, 35°C, 20 Ω, 0.2 mH, and, 100 μF, State 7 is 1000 W/m^2, 35°C, 20 Ω, 0.3 mH, and 100 μF. All of the states described are inspired by daily load, temperature, and irradiance changes. Here three different combination conditions like both irradiances and temperature varying; irradiances, temperature and load varying; irradiances, temperature, load, inductance, and capacitance varying are used to verify the controller robustness.

The ideal power and the PV power generated from the suggested MPPT approach under changing irradiance (Figure 14(a)) and temperature (Figure 14(b)) signals are shown in Figure 15. As per Figure 15, the proposed scheme is capable of tracking the MPP. The embedded zoom view in Figure 15 shows that the P_{PV} is capable of tracking the P_{ideal} under sudden changes in irradiance and temperature. The time duration to capture MPP is 0.002 sec.

The ideal power and the PV power achieved from the suggested MPPT approach under changing irradiance (Figure 14(a)), temperature (Figure 14(b)), and load (Figure 14(c)) signal are shown in Figure 16. The time duration to capture MPP is 0.004 sec. The PV current, PV voltage, Output current, and output voltage achieved from the suggested MPPT approach under simultaneously changing irradiance, temperature, and load signal are shown in Figure 17.

The ideal power and the PV power achieved from the suggested MPPT under simultaneously varying irradiance (Figure 14(a)), temperature (Figure 14(b)), load (Figure 14(c)), inductance (Figure 14(d)), and capacitance (Figure 14(e)) signal are shown in Figure 18. According to Figure 18, the suggested scheme is capable of tracking the MPP. The embedded zoom view in Figure 18 shows that the P_{PV} can track the P_{ideal} even when all five parameters change simultaneously. The time to capture MPP is 0.0015 sec.

The PV current, PV voltage, Output current, and output voltage achieved from the suggested MPPT method under simultaneously varying irradiance, temperature, load, inductance, and capacitance signal are shown in Figure 19.

The proposed MPPT scheme's performance is validated experimentally using a laboratory-based OPAL-RT real-time simulator (OP-4510) as displayed in Figure 20. It is a four-core real-time simulator. One of the features of this simulator is the RT-LAB system. It is divided into two sections. The first is the host computer, and the second is the RT simulator. Edits are made on the host computer. RT-LAB compiles the Simulink model and provides a user interface. The real-time model execution is handled by the RT simulator. It runs with the REDHAT operating system and communicates with the host via telnet.

The Simulink model was built in a real-time OPAL-RT environment and executed using the OPAL-RT (OP-4510) simulator. The signal such as V_{pv}, I_{pv}, and P_{pv} have been observed on DSO. The experimental results for P_{pv}, I_{pv}, and V_{pv} for the proposed controller are shown in Figure 21.

The proposed control method, as shown in Figure 21, tracks the MPP with low oscillations at any irradiation level. Furthermore, the MPP is accurately tracked when the radiation level changes abruptly from 350 W/m^2 to 600 W/m^2.

$$\text{Tracking efficiency} = \frac{P_{ideal} - P_{PV}}{P_{ideal}}, \tag{26}$$

$$\text{Overall system efficiency} = \frac{P_{ideal} - P_{out}}{P_{ideal}}. \tag{27}$$

The tracking efficiency and the overall system efficiency are calculated by the above equations. The tracking and overall system efficiency of the proposed controller are 99.8% and 96.1% respectively under changing irradiation conditions and it is illustrated in Figure 22(a)

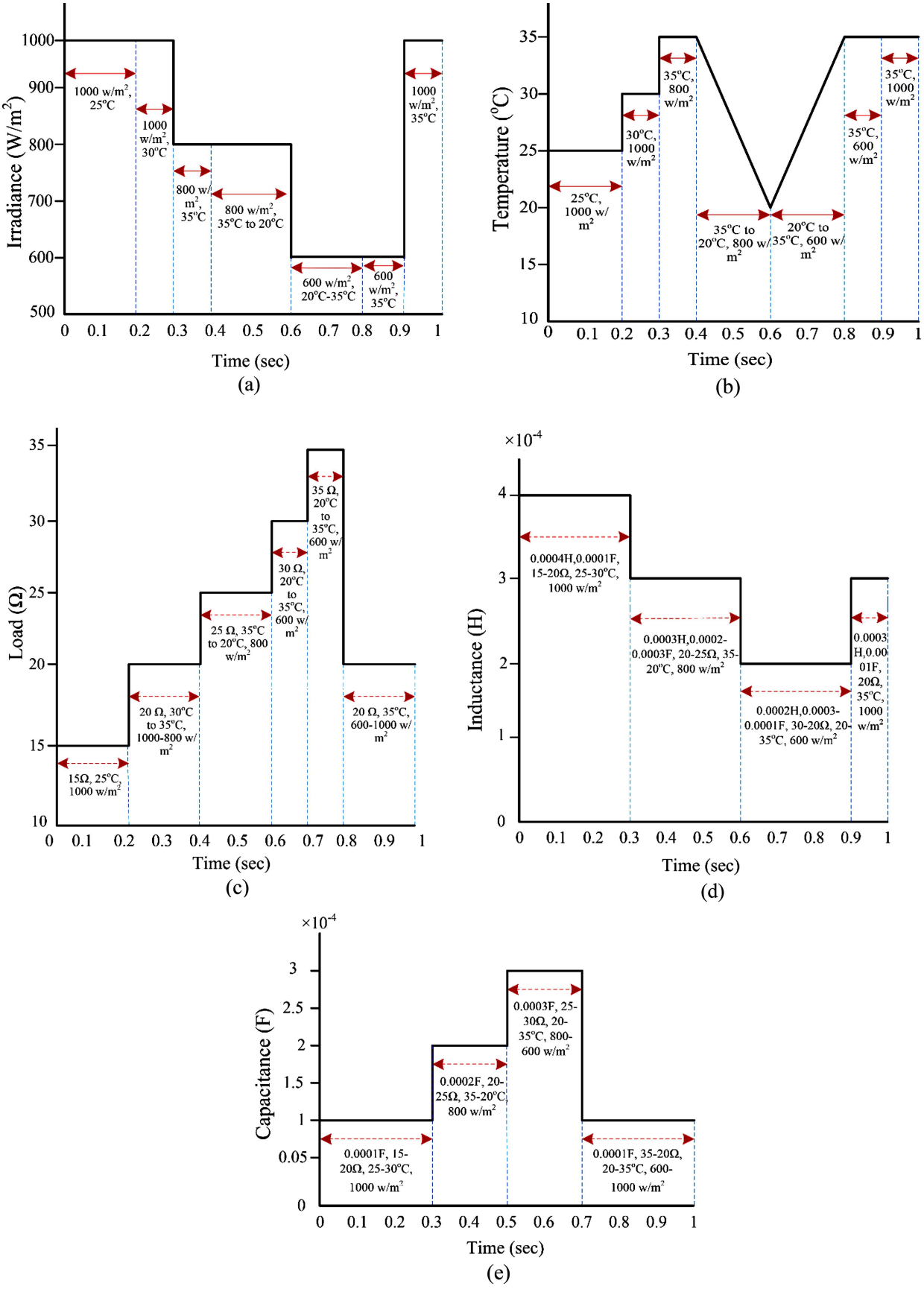

Figure 14. Signal of variable (a) irradiance, (b) temperature, (c) load, (d) inductance, and (e) capacitance.

and (b). The proposed approach performed the best under all of the varied climate conditions.

The tracking and overall system efficiency of the proposed controller are 99.75% and 96% respectively under simultaneously changing five different parameters and it is illustrated in Figure 23(a) and (b). The proposed approach performed the best under all of the varied climate conditions.

Table 4 shows the comparison of various recent MPPT algorithms with the novel RMRAC technique. It can clearly be seen that none of the exiting controller

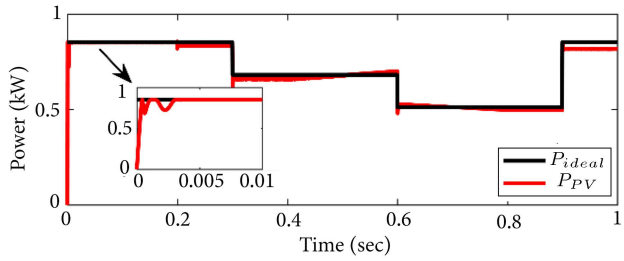

Figure 15. The ideal and PV power under varying irradiance and temperature signal.

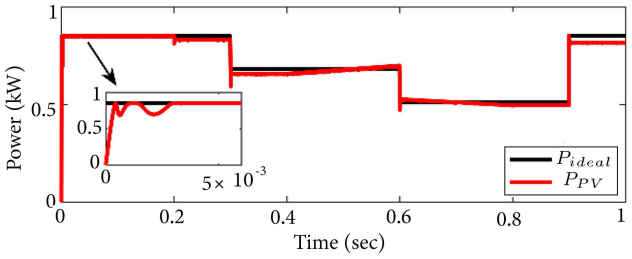

Figure 16. The ideal and PV power under simultaneously changing irradiance, temperature, and load signal.

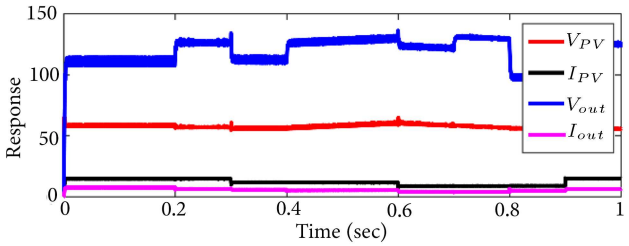

Figure 17. The PV current, PV voltage, Output current, and output voltage achieved from the suggested MPPT method under simultaneously changing irradiance, temperature, and load signal.

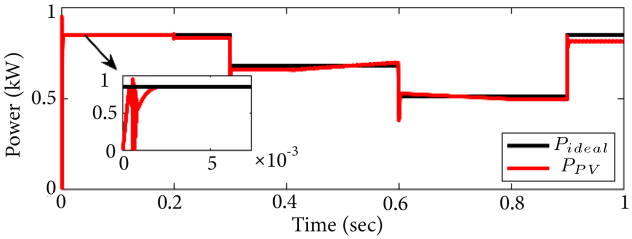

Figure 18. The ideal and PV power under simultaneously varying irradiance, temperature, load, inductance, and capacitance signal.

Table 4. The comparison of RMRAC with exiting popular algorithm.

MPPT technique	Tracking time under varying				Tracking efficiency
	Irradiation	Irradiation & temp.	Irradiation, temp. & load	Five parameter variations	
P&O [4]	0.28 sec	0.086 sec	–	–	91%–98%
INC [4]	0.24 sec	0.11 sec		–	96%–99%
FLC [4]	0.17 sec	0.027 sec	–	–	98.8%–99.4%
Adaptive FLC [4]	–	0.021 sec	–	–	99.5%–99.9%
BS-SMC [22]	–	0.011 sec	–	–	99.4%
PI [22]	–	0.048 sec	–	–	98%
iRCS-MPC [23]	0.006 sec	–	–	–	–
P&O-MPC [23]	0.026 sec	–	–	–	–
ANFIS [21]	0.125 sec	–	–	–	–
BAT-FLC [24]	0.12 sec	–	–	–	99.16%
SMC [32]	–	0.05 sec	–	–	99.10%
IPID MPPT [25]	0.6 sec	–	–	–	99.3%
Novel RMRAC	**0.005 sec**	**0.002 sec**	**0.004 sec**	**0.0015 sec**	**99.75%**

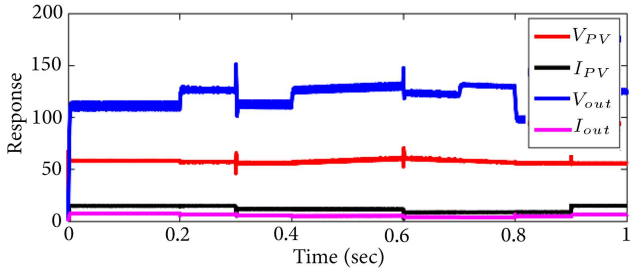

Figure 19. The PV current, PV voltage, output current, and output voltage under simultaneously varying irradiance, temperature, load, inductance, and capacitance signal.

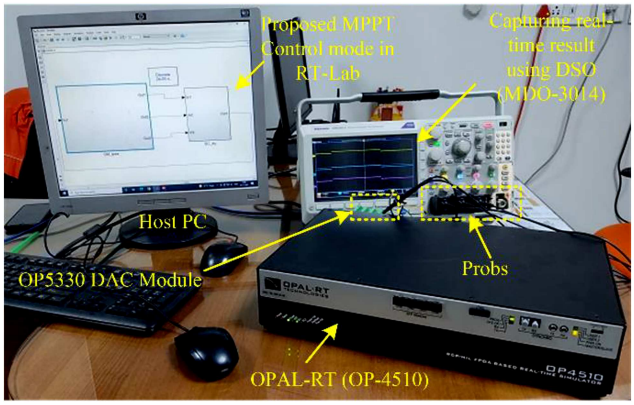

Figure 20. Experimental setup for real-time validation of proposed method using OPAL-RT simulator (OP-4510).

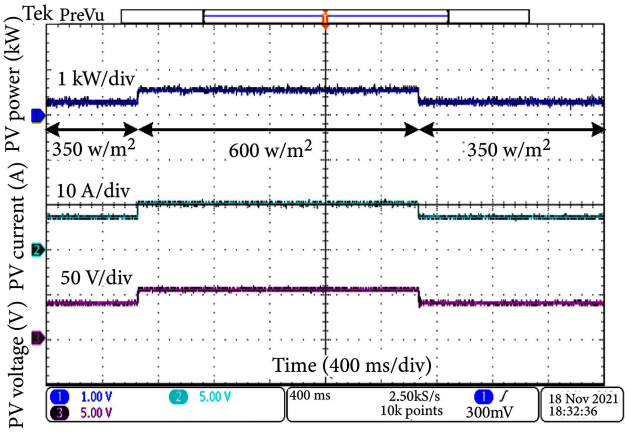

Figure 21. Experimental response of PV power, current, and voltage for the proposed method.

is able to track MPP after varying all five parameters simultaneously. It can also be seen that the tracking time of novel RMRAC is so much impressive. The bar plot of the tracking time under varying solar radiation and varying irradiation with temperature are shown in Figure 24.

The result demonstrates that the new MPPT technique for capturing MPP is the fastest and has the lowest oscillation rate at MPP, which implies the least amount of power loss. Also, the experimentally obtained results are close to the simulation results, indicating the proposed scheme is effective and feasible.

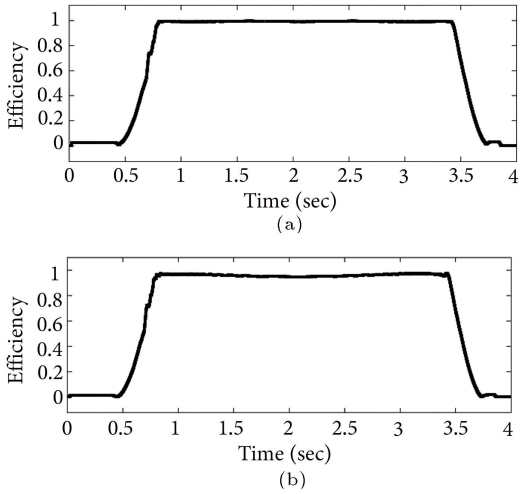

Figure 22. Efficiency (a) tracking and (b) overall system under varying irradiation condition.

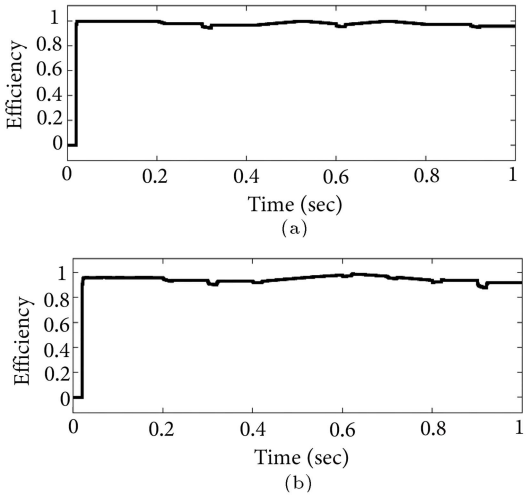

Figure 23. Efficiency (a) tracking and (b) overall system under varying five different parameters condition.

6. Conclusion

Adaptive control techniques are used extensively in time-changing or nonlinear systems due to their capability to adapt unpredictable changes in input or system dynamics. Furthermore, adaptive controllers often took less system previous knowledge and computing time. This research proposes a novel RMRAC-MPPT approach for PV systems under five different cases including temperature, irradiance, load, boost converter capacitance as well as inductance. To assess the robustness of the suggested method, MATLAB/Simulink software was utilized to compare it to well-established techniques such as P&O, INC, FLC, AFLC, SMC, back stepping-SMC, PI, iRCS-MPC,

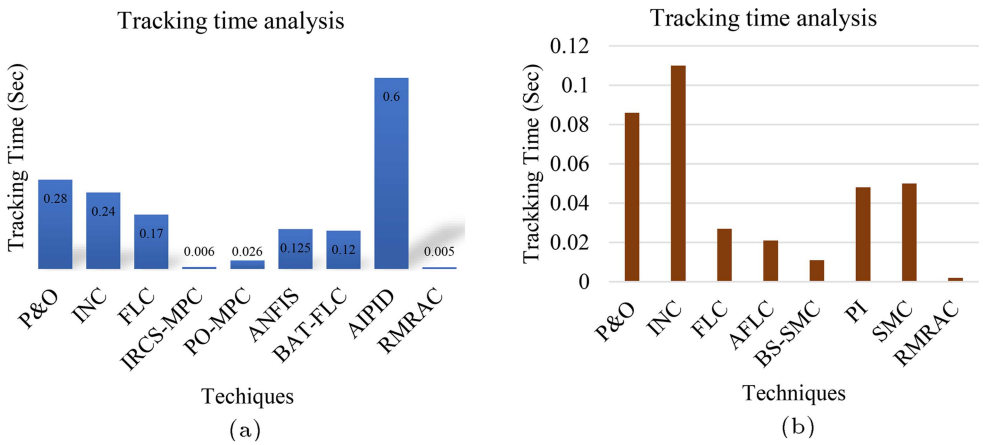

Figure 24. Bar plot (a) tracking time under varying irradiation and (b) tracking time under varying temperature and irradiation.

P&O-MPC, ANFIS, BAT-FLC, and IPID (incremental proportional integral derivative). The verification of the proposed method is also tested in a laboratory-based OPAL-RT real-time simulator. The proposed MPPT technique outperforms previous methods for determining Maximum Power Point (MPP) under rapid changes in system characteristics and atmospheric operating conditions. The tracking and overall system efficiency of the suggested MPPT are 99.75% and 96% respectively. In comparison to frequently utilized techniques, the suggested MPPT method produced the lowest oscillation rate at the MPP. This elevates the technique to the top of the efficiency rankings. According to the simulation results, the suggested MPPT approach takes 5 ms under radiation variation, 2 ms under both temperature and radiation variation, 4 ms under simultaneously varying load, temperature, and radiation, and 1.5 ms under simultaneously varying all five parameters to attain a steady-state. This indicates that the proposed MPPT approach is the best in terms of speed. Simultaneously, the amount of oscillation is relatively minimal as compared to traditional techniques. The suggested approach has a high level of accuracy and is also simple to implement in the system. Future work might concentrate on the effect of partial shading conditions as well as grid integration.

References

1. Agathokleous, R.A. and Kalogirou, S.A. "Status, barriers and perspectives of building integrated photovoltaic systems", *Energy*, **191**, 116471 (2020). DOI: 10.1016/j.energy.2019.116471
2. Martinopoulos, G. "Are rooftop photovoltaic systems a sustainable solution for Europe? A life cycle impact assessment and cost analysis", *Applied Energy*, **257**, 114035 (2020). https://doi.org/10.1016/j.apenergy.2019.114035
3. Refaat, A., Osman, M.H., and Korovkin, N.V. "Current collector optimizer topology to extract maximum power from non-uniform aged PV array", *Energy*, **195**, 116995 (2020). https://doi.org/10.1016/j.energy.2020.116995
4. Yilmaz, U., Turksoy, O., and Teke, A. "Improved MPPT method to increase accuracy and speed in photovoltaic systems under variable atmospheric conditions", *International Journal of Electrical Power and Energy Systems*, **113**, pp. 634–651 (2019). https://doi.org/10.1016/j.ijepes.2019.05.074
5. Bollipo, R.B., Mikkili, S., and Bonthagorla, P.K. "Critical review on PV MPPT techniques: Classical, intelligent and optimization", *IET Renewable Power Generation*, **14**(9), pp. 1433–1452 (2020). https://doi.org/10.1049/iet-rpg.2019.1163
6. Bhan, V., Hashmani, A., and Shaikh, M. "A new computing perturb-and-observe-type algorithm for MPPT in solar photovoltaic systems and evaluation of its performance against other variants by experimental validation", *Scientia Iranica*, **26**(6), pp. 3656–3671 (2019). DOI: 10.24200/sci.2019.54183.3635
7. Kumar, N., Hussain, I., Singh, B., et al. "Self-adaptive incremental conductance algorithm for swift and ripple free maximum power harvesting from PV array", *IEEE Transactions on Industrial Informatics*, **14**(5), pp. 2031–2041 (2018). DOI: 10.1109/TII.2017.2765083
8. Douiri, M.R. "Particle swarm optimized neuro-fuzzy system for photovoltaic power forecasting model", *Solar Energy*, **184**, pp. 91–104 (2019). https://doi.org/10.1016/j.solener.2019.03.09
9. Rezk, H., Aly, M., Al-Dhaifallah, M., et al. "Design and hardware implementation of new adaptive fuzzy logic-based MPPT control method for photovoltaic applications", *IEEE Access*, **7**, pp. 106427–106438 (2019). DOI: 10.1109/ACCESS.2019.2932694
10. Elnozahy, A., Yousef, A.M., Abo-Elyousr, F.K., et al. "Performance improvement of hybrid renewable energy sources connected to the grid using artificial neural network and sliding mode control", *Journal*

of Power Electronics, **21**, pp. 1166–1179 (2021). https://doi.org/10.1007/s43236-021-00242-8

11. Huang, Y.P., Chen, X., and Ye, C.E. "A hybrid maximum power point tracking approach for photovoltaic systems under partial shading ocnditions using a modified genetic algorithm and the firefly algorithm", *International Journal of Photoenergy*, **2018**, 7598653 (2018). https://doi.org/10.1155/2018/7598653

12. Harrag, A. and Messalti, S. "IC-based variable step size neuro-fuzzy MPPT improving PV system performances", *Energy Procedia*, **157**, pp. 363–374 (2019). https://doi.org/10.1016/j.egypro.2018.11.201

13. Pan, Z., Quynh, N.V., Ali, Z.M., et al. "Enhancement of maximum power point tracking technique based on PV-battery system using hybrid BAT algorithm and fuzzy controller", *Journal of Cleaner Production*, **274**, 123719 (2020). https://doi.org/10.1016/j.jclepro.2020.123719

14. Bhattacharyya, S., Kumar P, D.S., Samanta, S., et al. "Steady output and fast tracking MPPT (SOFT-MPPT) for P&O and InC algorithms", *IEEE Transactions on Sustainable Energy*, **12**(1), pp. 293–302 (2021). DOI: 10.1109/TSTE.2020.2991768

15. Kavya, M. and Jayalalitha, S. "A novel coarse and fine control algorithm to improve Maximum Power Point Tracking (MPPT) efficiency in photovoltaic system", *ISA Transactions*, **121**, pp. 180–190 (2022). https://doi.org/10.1016/j.isatra.2021.03.036

16. Charaabi, A., Zaidi, A., Barambones, O., et al. "Implementation of adjustable variable step based backstepping control for the PV power plant", *International Journal of Electrical Power & Energy Systems*, **136**, 107682 (2022). https://doi.org/10.1016/j.ijepes.2021.107682

17. Aminnejhad, H., Kazeminia, S., and Aliasghary, M. "Robust sliding-mode control for maximum power point tracking of photovoltaic power systems with quantized input signal", *Optik*, **247**, 167983 (2021). https://doi.org/10.1016/j.ijleo.2021.167983

18. Laxman, B., Annamraju, A., Srikanth, N.V. "A grey wolf optimized fuzzy logic based MPPT for shaded solar photovoltaic systems in microgrids", *International Journal of Hydrogen Energy*, **46**(18), pp. 10653–10665 (2021). https://doi.org/10.1016/j.ijhydene.2020.12.158

19. Srinivasarao, P., Peddakapu, K., Mohamed, M.R., et al. "Simulation and experimental design of adaptive-based maximum power point tracking methods for photovoltaic systems", *Computers & Electrical Engineering*, **89**, 106910 (2021). https://doi.org/10.1016/j.compeleceng.2020.106910

20. Verma, P., Garg, R., and Mahajan, P. "Asymmetrical fuzzy logic control-based MPPT algorithm for standalone photovoltaic systems under partially shaded conditions", *Scientia Iranica*, **27**(6), pp. 3162–3174 (2020). DOI: 10.24200/SCI.2019.51737.2338

21. Haji, D. and Naci, G. "Dynamic behaviour analysis of ANFIS based MPPT controller for standalone photovoltaic systems", *International Journal of Renewable Energy Research*, **10**(1), pp. 101–108 (2020). https://doi.org/10.20508/ijrer.v10i1.10244.g7897

22. Bjaoui, M., Khiari, B., Ridha, B., et al. "Practical implementation of the backstepping sliding mode controller MPPT for a PV-storage application", *Energies*, **12**(18), 3539 (2019). https://doi.org/10.3390/en12183539

23. Hussain, A., Sher H.A., Murtaza, A.F., et al. "Improved restricted control set model predictive control (iRCS-MPC) based maximum power point tracking of photovoltaic module", *IEEE Access*, **7**, pp. 149422–149432 (2019). DOI: 10.1109/ACCESS.2019.2946747

24. Ge, X., Ahmed, F.W., Rezvani, A., et al. "Implementation of a novel hybrid BAT-Fuzzy controller based MPPT for grid-connected PV-battery system", *Control Engineering Practice*, **98**, 104380 (2020). https://doi.org/10.1016/j.conengprac.2020.10438

25. Subudhi, B. and Pradhan, R. "A new adaptive maximum power point controller for a photovoltaic system", *IEEE Transactions on Sustainable Energy*, **10**(4), pp. 1625–1632 (2019). DOI: 10.1109/TSTE.2018.2865753

26. Salim, M.B., Hayajneh, H.S., Mohammed, A., et al. "Robust direct adaptive controller design for photovoltaic maximum power point tracking application", *Energies*, **12**(16), 3182 (2019). https://doi.org/10.3390/en12163182

27. Sahu, P. and Dey, R. "An improved 2-level MPPT scheme for photovoltaic systems using a novel high-frequency learning based adjustable gain-MRAC controller", *Scientific Reports*, **11**, 23131 (2021). https://doi.org/10.1038/s41598-021-02586-4

28. Khanna, R., Zhang, Q., Stanchina, W.E., et al. "Maximum power point tracking using model reference adaptive control", *IEEE Transactions on Power Electronics*, **29**(3), pp. 1490–1499 (2014). DOI: 10.1109/TPEL.2013.2263154

29. Sahu, P. and Dey, R. "Maximum power point tracking using adjustable gain based model reference adaptive control", *Journal of Power Electronics*, **22**, pp. 138–150 (2022). https://doi.org/10.1007/s43236-021-00336-3

30. Bhunia, M., Subudhi, B., and Ray, P.K. "Design and real-time implementation of cascaded model reference adaptive controllers for a three-phase grid-connected PV system", *IEEE Journal of Photovoltaics*, **11**(5), pp. 1319–1331 (2021). DOI: 10.1109/JPHOTOV.2021.3093047

31. Hasanien, H.M. "An adaptive control strategy for low voltage ride through capability enhancement of grid-connected photovoltaic power plants", *IEEE Transactions on Power Systems*, **31**(4), pp. 3230–3237 (2016). DOI: 10.1109/TPWRS.2015.2466618

32. Chaibi, Y., Salhi, M., and El-Jouni, A. "Sliding mode controllers for standalone PV systems:

modeling and approach of control", *International Journal of Photoenergy*, **2019**, 5092078 (2019). https://doi.org/10.1155/2019/5092078

Biographies

Saibal Manna received the M.Tech degree in Control and Automation from VIT, Vellore, India in 2019. Currently, he is pursuing PhD degree at the Department of Electrical Engineering, NIT Jamshedpur, Jharkhand, India. His research interests include adaptive control, optimal control, renewable energy, active suspension system, modern control system and machine learning.

Deepak Kumar Singh received the M.Tech degree in Control System from the BIT SINDRI, India, in 2019. He is currently pursuing Ph.D. degree in the Department of Electrical Engineering, NIT Jamshedpur, Jharkhand, India. His research interests include control system and renewable energy resources.

Ashok Kumar Akella was born in India, received the BSc (Engineering) and M.Tech (Control System) degrees from MIT Muzaffarpur, India in 1987 and 1992, respectively, completed his PhD (Renewable Energy System) from IIT Roorkee, India in 2006. He is a life member of ISTE. Since 1996, he has been serving as a faculty member at the Department of Electrical Engineering, NIT Jamshedpur, Jharkhand, India. His main research interests are control system, renewable energy system, and power quality.

Almoataz Y. Abdelaziz received the BSc and MSc degrees in Electrical Engineering from Ain Shams University, Cairo, Egypt in 1985 and 1990, respectively and PhD degree in Electrical Engineering according to the channel system between Ain Shams University, Egypt, and Brunel University, U.K., in 1996. He is currently a Professor of Electrical Power Engineering at Ain Shams University. Dr. Abdelaziz is the Chair of IEEE Education Society chapter in Egypt, a senior editor of Ain Shams Engineering Journal, an editor of Electric Power Components and Systems Journal, a member of editorial board, and a reviewer of technical papers in several international journals and conferences. He is a senior member in IEEE, a member in IET, and a part of Egyptian Sub-Committees of IEC and CIGRE. He has been awarded many prizes for distinct research and for international publishing from Ain Shams University, Egypt. He has authored or coauthored more than 300 refereed journal and conference papers in his research areas, which include the applications of artificial intelligence as well as evolutionary and heuristic optimization techniques to power system operation, planning, and control.

Miska Prasad was born in India and received BE in Electrical and Electronics Engineering from GITAM University, Andhra Pradesh, India, and M.Tech in Power Systems from NIT Jamshedpur, Jharkhand, India in 2010 and 2013, respectively. He completed PhD degree from Electrical Engineering Department, NIT Jamshedpur, India in 2019. Currently, he is an Associate professor in the Department of Electrical and Electronics Engineering, ACE Engineering College, Telangana, India. His main research interests are power quality, custom power devices, and power electronics.